New mixed ligand oxorhenium(V) complexes of 3-thiapentane-1,5-dithiolato with 2-thiocytosine and 5-amino-1,3,4-thiadiazole-2-thiol: Experiment and theory

ARTICLE *in* INORGANICA CHIMICA ACTA · JANUARY 2015

Impact Factor: 2.05 · DOI: 10.1016/j.ica.2014.10.004

6 AUTHORS, INCLUDING:

Arnab Bhattacharya
Tripura University
11 PUBLICATIONS **17** CITATIONS
SEE PROFILE

Smita Majumder
Tripura University
7 PUBLICATIONS **17** CITATIONS
SEE PROFILE

Rakesh Ganguly
Nanyang Technological University
102 PUBLICATIONS **567** CITATIONS
SEE PROFILE

Shubhamoy Chowdhury
Tripura University
41 PUBLICATIONS **331** CITATIONS
SEE PROFILE

Inorganica Chimica Acta 425 (2015) 124–133

Contents lists available at ScienceDirect

Inorganica Chimica Acta

journal homepage: www.elsevier.com/locate/ica

New mixed ligand oxorhenium(V) complexes of 3-thiapentane-1,5-dithiolato with 2-thiocytosine and 5-amino-1,3,4-thiadiazole-2-thiol: Experiment and theory

Arnab Bhattacharya [a], Jnan Prakash Naskar [b], Smita Majumder [a], Rakesh Ganguly [c], Partha Mitra [d], Shubhamoy Chowdhury [a,*]

[a] Department of Chemistry, Tripura University, Suryamaninagar, Tripura 799 022, India
[b] Department of Chemistry, Inorganic Chemistry Section, Jadavpur University, Jadavpur, Kolkata 700 032, India
[c] Division of Chemistry & Biological Chemistry, SPMS-CBC-01-18D, Nanyang Technological University, 21 Nanyang Link, Singapore 637371, Singapore
[d] Department of Inorganic Chemistry, Indian Association for the Cultivation of Science, Jadavpur, Kolkata 700 032, India

ARTICLE INFO

Article history:
Received 16 July 2014
Received in revised form 9 September 2014
Accepted 3 October 2014
Available online 12 October 2014

Keywords:
Oxorhenium(V) complexes
Electrochemistry
DFT
TD-DFT

ABSTRACT

By using η^3-($SCH_2CH_2SCH_2CH_2S$) (SSS), 2-thiocytosine (HL^1) and 5-amino-1,3,4-thiadiazole-2-thiol (HL^2) as S-donor ligands two '3 + 1' mixed ligand red oxorhenium(V) complexes of the type $[ReO(SSS)(HL^1)]Cl$ (**1**Cl) and $[ReO(SSS)(L^2)]$ (**2**) have been synthesized. Both **1**Cl and **2** have been characterized by C, H and N microanalyses, ^1H NMR, FT-IR, UV–Vis spectra and conductivity measurements. The X-ray crystal structures of both **1**Cl and **2** have been determined. Electrochemical studies of **1**Cl in acetonitrile show four successive one-electron redox couples; while **2** in DMSO displays only two one- electron redox steps. A computational and conceptual Density Functional Theory (DFT) studies have been performed on various (3 + 1) complexes of Re(V). The fully-optimized complexes, **1**Cl and **2,** adopt geometries that satisfactorily corroborate the X-ray structures. Subsequently these optimized structures were employed to investigate systematically the relative stabilities of various Re(V) complexes with varying ligands having N, O and S donor atoms. The electronic properties of **1**Cl and **2** were delved into employing the hybrid STMP TD-DFT method and the results were found to be in good harmony with the experimental observations.

1. Introduction

^{99m}Tc, the most widely used radionuclide for diagnostic imaging in nuclear medicine, is a chemical congener of rhenium. Consequently the chemistry of rhenium is almost akin to that of technetium. These aspects have propelled the interest in rhenium chemistry by its ever growing scope in playing the pivotal role in the synthesis of radiopharmaceuticals suitable for diagnostic and therapeutic agents [1–3]. The isotopes of rhenium have attractive and compatible nuclear properties for diagnostic and therapeutic purposes in nuclear medicine [4]. For ready reckoning, ^{186}Re have E_{max} of 1.070 MeV for β-emission and E_{max} of 0.137 MeV for γ-emission with $t_{½}$ = 90 h; while for ^{188}Re: E_{max} = 2.120 MeV for β-emission and E_{max} = 0.155 MeV for γ-emission with $t_{½}$ = 17 h.

Generally for rhenium compounds, integrated or bi-functional approaches have been used for drug designing [2,5]. In this perspective, '3 + 1' mixed ligand approach has been attempted for developing novel radiopharmaceuticals with oxo-Re(V). Here the ReO^{3+} core is coordinated with tri-dentate dithiolates (SES, E = O, S or NR) and uni-dentate thiolates. Much attention has been paid to this approach [6] owing to the consideration that oxo-Re(V) complexes with '3 + 1' mixed ligands enable the coupling of biologically relevant groups and molecules. The neutral nature of such species also finds suitable application in the modeling of Tc and Re based neuro-receptor complexes [7]. Such complexes can easily be prepared through reactions of $[ReOX_4]^-$ with tri-dentate ligand followed by the addition of mono-dentate ligands in a one-pot synthesis [8].

In the present work we have chosen two mono-dentate heterocyclic amino thiolates, 2-thiocytosine (HL^1) and 5-amino-1,3,4-thiadiazole-2-thiol (HL^2), as ligands. 2-thiocytosine has already been studied for its effects on mitosis and DNA synthesis of cultured human lymphocytes [9]. It is used as inhibitors of cytosine deaminase [10] and is also used to generate structure-free DNA [11]. The ligand, 5-amino-1,3,4-thiadiazole-2-thiol (HL^2), has recently been found electrochemical applications in surface modified electrode for determination of epinephrine [12] and as sensors

* Corresponding author. Fax: +91 381 2374802.
E-mail address: shubha103@yahoo.com (S. Chowdhury).

http://dx.doi.org/10.1016/j.ica.2014.10.004
0020-1693/

for DNA [13]. Again, a few of its complexes are cytotoxic agents [14] while some are used for the stabilization of gold nanoparticles [15].

For quite some time oxorhenium complexes have also been studied to know their electronic structures and bonding situations using DFT [16]. A large number of systems containing the oxorhenium core have been studied by Gancheff et al. [17–19], assimilating the information regarding the interaction of amino and thiolato groups attached to rhenium. Other systems with neutral N donor ligands have been studied by Machura et al. [20,21]. Time-Dependent DFT studies have been made the part of this investigation for explaining the electronic structures of oxorhenium species as well as in the prediction of reaction pathways to correlate the energetics of the reactions. This understanding is crucial particularly for the catalytic aspects of oxorhenium complexes [22,23]. These extensive studies, however, do not encompass the oxorhenium complexes of (3 + 1) type. Curiously one lone report [24] assesses the relative stabilities of various tri-dentate ligands in the oxo-Re(V) system.

In this context, we wish to report our individual reactions of [ReO(SSS)Cl] with HL^1 and HL^2 to have an ionic complex, [ReO(SSS)(HL^1)]Cl (**1**Cl) and a neutral complex, [ReO(SSS)(L^2)] (**2**) having '$ReOS_4$' core. The molecular structures and electrochemical properties of both **1**Cl and **2** have been delved into. To the best of our knowledge, there is no report on the studies of reaction energy (ΔE) on mixed ligand '3 + 1' four sulfur containing '$ReOS_4$' core with tri-dentate thiadithiolate (SSS) ligand and a mono-dentate thiolate ligand. This prompted us to undertake experimental and theoretical studies to analyze the nature of these '3 + 1' systems.

2. Experimental

2.1. Materials and measurements

All chemicals were of analytical reagent grade and used without further purification. 2-thiocytosine (HL^1), 5-amino-1,3,4-thiadiazole-2-thiol (HL^2) and 3-thiapentane-1,5-dithiolato were procured from Sigma–Aldrich, USA. The chloro(3-thiopentane-1,5-dithiolato)oxorhenium(V) complex, [ReO(SSS)Cl], was prepared following a reported procedure [6a]. Microanalyses were performed with a Perkin–Elmer 2400II elemental analyzer. FT-IR spectra were recorded as KBr pellets with a Perkin-Elmer FT-IR-100 spectrophotometer. UV–Vis absorption spectra of the complexes, **1**Cl and **2** were recorded on a Perkin–Elmer Lambda 25 spectrophotometer. Solution electric conductivity measurements were carried out for **1**Cl in CH_3OH and for **2** in DMSO at room temperature on a Systronics (India) direct reading conductivity meter (Model: 304). Cyclic voltammetric (CV) data were acquired on a Bioanalytical Systems Inc. Epsilon electrochemical workstation (Model: CV-50) on a C3 cell stand at 293 K. Dry and degassed acetonitrile solution for **1**Cl and DMSO for **2**, each of which contained ~1.0 mM of analyte and 0.10 M tetra-*n*-butyalammonium perchlorate (TBAP) as supporting electrolyte, were saturated with nitrogen for 15 min prior to each acquisition. A blanket of nitrogen gas was maintained throughout the measurements. The measurements were carried out with a three-electrode assembly comprising a Glassy Carbon (GC) working electrode, a platinum wire counter electrode and a Ag/AgCl reference electrode. The working electrode was polished with alumina slurry before each acquisition. All potentials reported herein are referenced to Ag/AgCl.

2.2. Preparation of complex [ReO(SSS)(HL^1)]Cl (**1**Cl)

Acetonitrile solution (10 ml) containing HL^1 (0.043 g, 0.33 mmol) was added dropwise to acetonitrile solution (15 ml) containing [ReO(SSS)Cl] (0.129 g, 0.33 mmol) at room temperature. Initially the mixture was stirred for 1 h and subsequently refluxed for 3 h. A red solution was obtained thereby. It was evaporated under reduced pressure to have a red mass (yield: 0.135 g, 78%). *Anal.* Calc. for $C_8H_{13}N_3ORe S_4Cl$ (mol. wt. 517.13): C, 18.58; H, 2.53; N, 8.13. Found: C, 18.42; H, 2.68; N, 7.97%. IR (KBr, cm^{-1}): 3290, 3213, (s, NH_2); 1658 (vs, C=N); 974 (s, Re=O); 765 (m, C–S). UV–Vis (MeOH, λ/nm, (ε/M^{-1} cm^{-1})): 506 (275), 371 (4 141), 260sh (21 772), 242 (31 967), 223 (22 025). ^{1}H NMR (DMSO-d_6, ppm): 2.73–2.83 (m, 2H, –CH_2–), 3.09–3.24 (m, 2H, –CH_2–), 4.16–4.25 (m, 2H, –CH_2–) 4.26–4.36 (m, 2H, –CH_2–), 6.57 (*d*, 1H, C*H* of pyrimidine ring), 8.10 (*d*, 1H, C*H* of pyrimidine ring), 8.66 (br. s, 2H, =NH_2^+). Λ_M (CH_3OH): 96 Ω^{-1} cm^2 mol^{-1} (1:1 electrolyte). The slow aerial evaporation of a moderately concentrated solution of the compound in CH_3OH afforded single crystals fit for X-ray crystal structure determination.

2.3. Preparation of complex [ReO(SSS)(L^1)] (**1a**)

An acetonitrile solution (10 ml) containing HL^1 (0.026 g, 0.20 mmol) was added dropwise to another acetonitrile solution (10 ml) containing [ReO(SSS)Cl] (0.078 g, 0.20 mmol) at room temperature. One drop of triethylamine was also added. The reaction mixture was stirred for 1 h to give rise a red solution. The resulting solution was allowed to evaporate naturally to get a red mass. After, the separated solid mass was filtered, washed thoroughly with water and dried in vacuo over fused $CaCl_2$ (yield: 0.060 g, 62%). *Anal.* Calc. for $C_8H_{12}N_3ORe S_4$ (mol. wt. 480.63): C, 19.99; H, 2.52; N, 8.74. Found: C, 19.87; H, 2.48; N, 8.79%. IR (KBr, cm^{-1}): 3424, 3312, (s, NH_2); 1653 (vs, C=N); 971 (s, Re=O); 775 (m, C–S). UV–Vis (MeOH, λ/nm, (ε/M^{-1} cm^{-1})): 504 (212), 374 (4 384), 273 (29 707), 242 (37 552), 214 (44 564). ^{1}H NMR (DMSO-d_6, ppm): 2.66–2.79 (m, 2H, –CH_2–), 3.05–3.22 (m, 2H, –CH_2–), 4.11–4.29 (m, 2H, –CH_2–) 4.22–4.35 (m, 2H, –CH_2–) 6.42 (*d*, 1H, C*H* of pyrimidine ring), 7.94 (*d*, 1H, C*H* of pyrimidine ring), 8.41 (br. s, 2H, –NH_2). Λ_M (CH_3OH): 0.14 Ω^{-1} cm^2 mol^{-1} (nonelectrolyte). In spite of our repeated attempts, we could not generate single crystals of **1a** fit for X-ray crystallography.

2.4. Preparation of complex [ReO(SSS)(L^2)] (**2**)

A dichloromethane solution (10 ml) containing HL^2 (0.027 g, 0.20 mmol) was added dropwise to a dichloromethane solution (10 ml) containing [ReO(SSS)Cl] (0.078 g, 0.20 mmol) at room temperature. One drop of triethylamine was also added. The resulting mixture was stirred for 15 min to give rise a red solution which was washed with water. Finally the solution was allowed to evaporate naturally to get a red mass. (yield: 0.081 g, 83%). *Anal.* Calc. for $C_6H_{10}N_3ORe S_5$ (mol. wt. 486.73): C, 14.81; H, 2.07; N, 8.63. Found: C, 15.22; H, 2.45; N, 8.84%. IR (KBr, cm^{-1}): 3402, 3252 (s, NH_2); 1615 (vs, C=N); 963 (s, Re=O); 762(m, C–S). UV–Vis (DMSO, λ/nm, (ε/M^{-1} cm^{-1})): 501 (410), 389(5 157), 270 (14 452). ^{1}H NMR (DMSO-d_6, ppm): 2.63–2.78 (m, 2H, –CH_2–), 3.01–3.23 (m, 2H, –CH_2–), 4.02–4.33 (m, 2H, –CH_2–) 4.24–4.33 (m, 2H, –CH_2–), 8.45 (br. s, 2H, –NH_2). Λ_M (DMSO): 0.61 Ω^{-1} cm^2 mol^{-1} (nonelectrolyte). The X-ray quality crystals were grown from a solution of **2** in DMSO under natural evaporation.

2.5. Crystal structures determination

Single crystals suitable for X-ray structure determination of the complexes, **1**Cl and **2,** were selected by examination under a microscope. The appropriate single crystals of **1**Cl and **2** were mounted on a Bruker SMART APEX II CCD area detector diffractometer at 150 (2) and 103(2) K respectively using graphite monochromated Mo Kα radiation (λ = 0.71073 Å). Intensity data of **1**Cl and **2**

were reduced using SAINT [25] and the empirical absorption corrections were performed with SADABAS package [26]. The structures of both **1**Cl and **2** were solved by direct methods and refined by full-matrix least-square methods based on $|F|^2$ using SHELXL-97 [27]. All non-hydrogen atoms were refined anisotropically. Hydrogen atoms were placed in calculated positions and constrained to ride on their parent atoms. All the calculations were carried out using SHELXS-97, SHELXL-97 and SHELXTL [27] programs. The crystallographic data for **1**Cl and **2** are summarized in Table 1.

2.6. Computational details

All computational studies were performed at the level of density functional theory (DFT). The geometry was optimized in a closed-shell singlet ($S = 0$) state starting from the molecular structure as determined by X-ray crystallography. In describing the Re–S bond the (2 + 2) mixed ligand systems; PBE1PBE in combination with the so-called STMIDI basis set, has been shown to reproduce Re–S bonds with very low computational cost [28]. Here we have assessed eight DFT methodologies to study structural and vibrational properties of our '3 + 1' mixed ligand complexes, **1**Cl and **2**. They are PBE1PBE, PBEPBE [29–31], MPW1PW91 [32] and TPSSTPSS [33] in combination with LANL2DZ and STMIDI. These DFT methods will be called STMP1 (PBE1PBE and STMIDI), LANP1 (PBE1PBE and LANL2DZ), STMP (PBEPBE and STMIDI), LANP (PBEPBE and LANL2DZ), STMM (MPW1PW91 and STMIDI), LANM (MPW1PW91 and LANL2DZ), STMT (TPSSTPSS and STIMIDI) and LANT (TPSSTPSS and LANL2DZ) respectively. For the metal atom, the core electrons (60) were treated through the pseudo-potential approximations (ECP) as included in the LANL2DZ [34] basis set. The valence electrons for the non-metal atoms in STMIDI were treated with MIDI, [35] those for the metal being described by a basis set (8s7p6d2f1g)/[6s5p3d2f1g] [36]. The core electrons were replaced by Stuttgart effective core pseudo-potentials [36,37]. These basis sets take relativistic effects into account. Such consideration is important specifically when systems with heavy atoms are studied [38]. Time-dependent DFT (TD-DFT) method was employed to calculate 70 singlet transitions both for **1**Cl and **2** in DMSO [39] solution, the latter being described by the conductor-like polarizable continuum model (C-PCM) [40,41]. Electronic spectra were simulated by means of the program package GAUSSIAN 09, Rev. C.01, [42]. The results were interpreted and plotted respectively by Gauss Sum [43] and Gabedit [44] softwares.

Table 1
Crystal data and structure refinement parameters for **1**Cl and **2**.

Parameter	**1**Cl	**2**
Formula	$C_8H_{13}N_3ORES_4.Cl.3H_2O$	$C_6H_{10}N_3ORES_5$
Formula weight	571.20	486.67
Crystal system	triclinic	triclinic
Space group	$P\bar{1}$	$P\bar{1}$
Unit cell dimensions		
a (Å)	7.404(3)	6.8334(3)
b (Å)	10.541(4)	10.3014(4)
c (Å)	12.009(5)	10.3742(4)
α (°)	86.386(7)	118.1947(10)
β (°)	73.738(7)	91.1298(12)
γ (°)	87.051(8)	100.5127(11)
V (Å^3)	897.4(6)	628.08(4)
Z	2	2
T (K)	150(2)	103(2)
ρ_{calc} (g/cm^3)	2.114	2.573
μ (Mo Kα) (mm^{-1})	7.399	10.485
F(000)	552	460
Crystal Size (mm)	0.11 × 0.16 × 0.25	0.12 × 0.14 × 0.24
λ (Mo Kα) (Å)	0.71073	0.71073
θ ranges (°)	1.8 < θ < 25.0	3.06 < θ < 31.2
Total reflection	8242	16697
Reflection independent (R_{int})	3156 (0.080)	4043 (0.0398)
$h/k/l$	−8, 8/−12, 12/−14, 14	−9, 9/−14, 14/−15, 15
Reflection observed (I > 2σ)	2836	3778
R_1	0.0545	0.0203
wR_2	0.1442	0.0441
Goodness of fit (GOF)	1.04	1.066
$\Delta\rho_{max}$ and $\Delta\rho_{min}$ (e Å^{-3})	2.86, −3.99	0.851, −0.866

$R_1 = \sum||F_o| - |F_c||/\sum|F_o|$, $wR_2 = [\sum w(F_o^2 - F_c^2)^2/\sum w(F_o^2)^2]^{1/2}$, calcd. $w = 1/[\sigma^2(F_o^2) + (0.0907P)^2 + 0.4301P]$ for **1**Cl and $w = 1/[\sigma^2(F_o^2) + (0.0180P)^2 + 0.0659P]$ for **2** where $P = (F_o^2 + 2F_c^2)/3$.

3. Results and discussion

3.1. Synthesis of the complexes

The oxorhenium(V) complexes under study, **1**Cl or **1a** and **2**, have been obtained out of the ligand exchange reaction of [ReO(SSS)Cl] with 2-thiocytosine (HL^1) and 5-amino-1,3,4-thiadiazole-2-thiol (HL^2) in equimolar proportions. **1**Cl has been prepared in acetonitrile milieu; while **1a** and **2** can be isolated from acetonitrile and dichloromethane solution respectively in presence of triethylamine as base. The complexes **1**Cl, **1a** and **2** were isolated as solid red masses. The C, H and N microanalytical data of the complexes **1**Cl, **1a** and **2** are consistent with our proposed empirical formulae. **1**Cl and **1a** are soluble in methanol, acetonitrile, DMSO, DMF but **2** is soluble only in DMSO and DMF. The room temperature (298 K) effective magnetic moments of the complexes are found to be diamagnetic in nature. **1**Cl is a 1:1 electrolyte in methanol. However, **1a** and **2** maintain its non-electrolytic nature in solution [45].

3.2. FTIR and ^{1}H NMR spectroscopy

The complexes, **1**Cl and **2** show strong peaks in their respective IR spectrum at 974 and 963 cm^{-1}, which are assigned to ν(Re=O) stretching. For **1a,** ν(Re=O) stretching appears at 971 cm^{-1}. These values match well with those (930–980 cm^{-1}) observed in other '3 + 1' oxo-Re(V) complexes [46–48]. The IR spectra of the complexes, **1**Cl, **1a** and **2** have very strong intensity bands at 1658, 1653 and 1615 cm^{-1} respectively. These bands are assigned to the stretching vibrations of C=N bonds of the ring [49]. The medium intensity stretching vibrations of the C–S bonds in **1**Cl and **2** can be discerned respectively at 765 and 762 cm^{-1} [46]. The strong N–H stretching vibrations of **1**Cl and **2** can be found at 3290, 3213 and 3402, 3252 cm^{-1} respectively [49].

^{1}H NMR signals of the substituted pyrimidine ring were observed as two doublets at 8.10 and 6.57 ppm for **1**Cl. The methylene proton signals in the chelate ring, SSS are strongly coupled with each other. Protons on the coordinated SSS are identified as *endo* (protons closer to oxygen of Re=O core) and *exo* (remote from oxygen atom of Re=O core) [8b,50]. The *endo* protons are more strongly deshielded than those of *exo* protons, because the *endo* protons interact more strongly with the π-cloud of Re=O. Therefore, ^{1}H NMR signals of *endo* protons should appear at lower field compared to the *exo* ones. The multiple signals in the ranges 4.24–4.36, 4.02–4.25, 3.01–3.24 and 1.63–2.83 ppm for complexes **1**Cl and **2** are assigned respectively as the endo-terminal, endo-inside, exo-terminal and exo-inside methylene protons, The difference in chemical shift values between the *endo*- and *exo*-methylene protons on the coordinated SSS is comparable with the literature values [8b,51]. Complete assignments of the ^{1}H NMR spectra for complexes, **1**Cl and **2** are given in Figs. S1 and S2.

3.3. Molecular structures

ORTEP diagrams with the atomic labeling scheme for **1**Cl·3H_2O and **2** are shown in Fig. 1. Selected metrical parameters for these complexes are tabulated in Table 2. As seen from Fig. 1, the coordination sphere of Re is completed by four sulfur donor atoms and one oxygen atom. The Re=O bond distances of **1**Cl and **2** are 1.681(2) and 1.694(2) Å, respectively. This marginal difference is also reflected in the Re=O stretching frequencies (974 cm^{-1} for **1**Cl and 963 cm^{-1} for **2**). The Re1–S4 bond distance (2.329 Å) of complex **2** is shorter than that of Re1–S5 (2.363 Å) of complex **1**Cl. This indicates that the basicity of HL^2 is stronger than that of HL^1. The bond lengths of Re–S are in the expected range and are comparable with other well-characterized rhenium complexes [8b,46,52].

The trigonality indices (τ [8b,46] of **1**Cl and **2** were evaluated based on the definition, $\tau = (\beta - \alpha)/60$, where β and α, respectively are the largest and second largest angles of the central metal atom with the surrounded donor atoms. τ value is equal to 0 for a regular

Table 2
Selected bond lengths (Å) and angles (°) for **1**Cl and **2**.

Bond lengths (Å)			
1Cl		**2**	
Re1–O1	1.681(8)	Re1–O1	1.694(2)
Re1–S1	2.373(3)	Re1–S2	2.3692(7)
Re1–S2	2.320(3)	Re1–S1	2.2906(7)
Re1–S4	2.315(2)	Re1–S3	2.2959(8)
Re1–S5	2.363(2)	Re1–S4	2.3289(7)
Bond angles (°)			
1Cl		**2**	
S1–Re1–S2	84.40(8)	S1–Re1–S2	84.18(2)
S1–Re1–S4	84.90(8)	S2–Re1–S3	84.32(3)
S1–Re1–S5	152.95(8)	S2–Re1–S4	154.22(3)
S1–Re1–O1	100.6(3)	S2–Re1–O1	101.04(7)
S2–Re1–S4	130.66(10)	S1–Re1–S3	127.63(3)
S2–Re1–S5	79.99(9)	S1–Re1–S4	87.12(3)
S2–Re1–O1	115.1(3)	S1–Re1–O1	116.39(8)
S4–Re1–S5	88.66(8)	S3–Re1–S4	81.91(3)
S4–Re1–O1	114.2(3)	S3–Re1–O1	115.95(8)
S5–Re1–O1	106.0(3)	S4–Re1–O1	104.57(7)

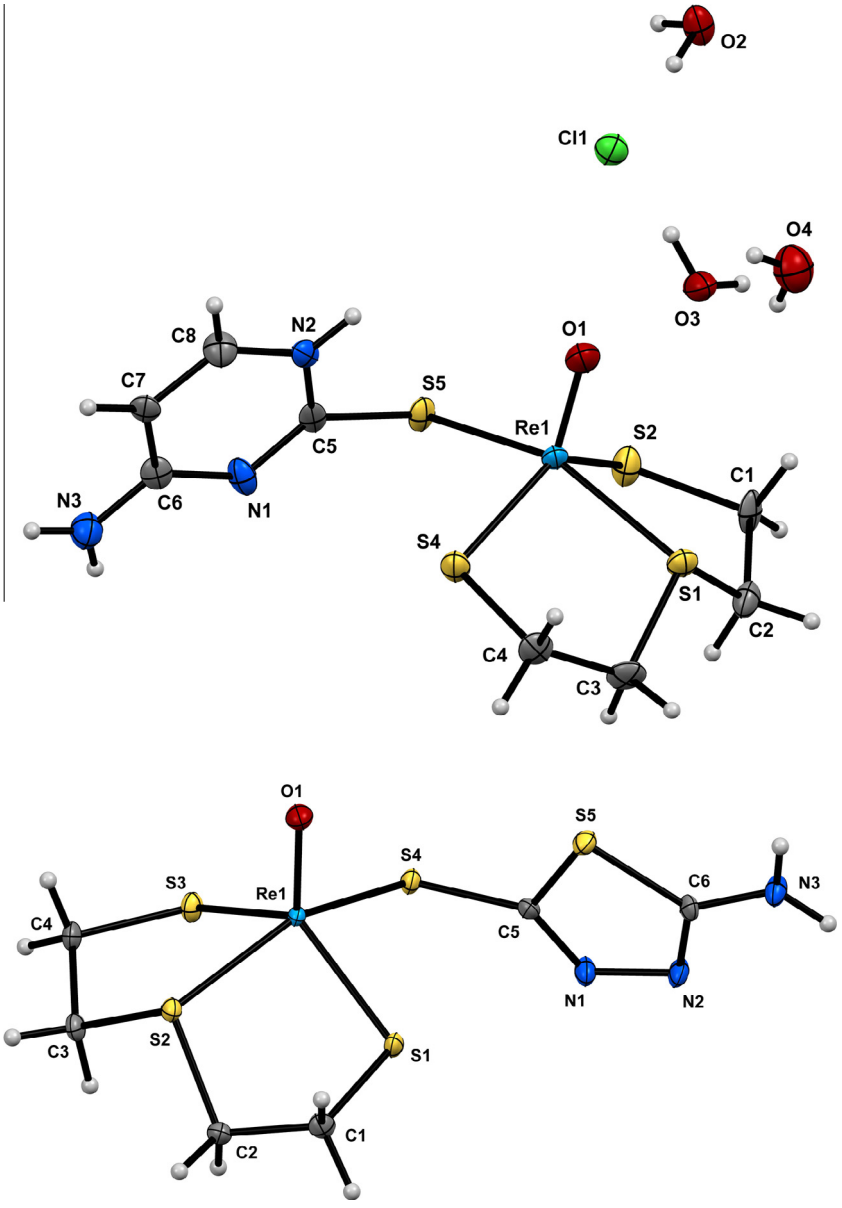

Fig. 1. ORTEP diagrams of complexes **1**Cl·3H_2O (top) and **2** (bottom) showing the atom-labeling scheme and 50% thermal ellipsoids.

Table 3
Hydrogen Bonds (Å, °) for **1**Cl and **2**.

1Cl				
D–H···A	D–H	H···A	D···A	D–H–A
N2–H2···O3	0.86	1.94	2.772(11)	164
O2–H2*a*···Cl1	0.82	2.50	3.246(8)	152
O2–H2*b*···Cl1	0.82	2.35	3.162(8)	168
N3–H3*b*···O2	0.86	2.07	2.891(12)	158
O3–H3*c*···Cl1	0.81	2.43	3.214(8)	163
O3–H3*d*···Cl1	0.82	2.41	3.184(8)	157
O4–H4*a*···O3	0.82	2.27	2.921(11)	137
2				
N3–H3*e*···N2	0.88	2.21	3.001(5)	149

a = −1 + *x*, *y*, *z*; *b* = 1 + *x*, *y*, *z*; *c* = 1 − *x*, 2 − *y*, 2 − *z*; *d* = 1 − *x*, 1 − *y*, 1 − *z*; *e* = 1 − *x*, 1 − *y*, 2 − *z*.

square pyramid. It is of unity for a regular trigonal bipyramidal geometry. For **1**Cl, ∠(S1–Re1–S5) = 152.95° (β) and ∠(S2–Re1–S4) = 130.66° (α) while for **2**, β [∠(S2–Re1–S4)] and α [∠(S1–Re1–S3)] are 154.22° and 127.63°, respectively. Accordingly the τ value for **1**Cl comes out 0.372. This value is of 0.443 for **2**. These values are suggestive of the distorted square pyramidal geometries both for **1**Cl and **2**. In **1**Cl, the rhenium center is displaced by 0.756 Å from the mean basal plane defined by four sulfur donor atoms. Similar displacement in **2** is 0.888 Å.

The crystal structure of **1**Cl·3H_2O is stabilized by O–H···Cl, N–H···O and O–H···O hydrogen bonds (Table 3). The solvate water molecules O2 and O3 as well as the counter anion Cl^- are hydrogen bonded to formed 1D chains, to which the complex molecules are hanged through N3···O2 and N2···O3 bonds, to finally give rise the 3D lattice structure. The crystal packing diagram illustrating the hydrogen bonding in **1**Cl·3H_2O is shown in Fig. 2. The crystal structure of **2** is also stabilized by N–H···N hydrogen bonds (Table 3) resulting a dimeric structure which is extended to 1D chain in the lattice by contacts with S3···S5 (3.527 Å) and S4···S5 (3.477 Å) shown in Fig. 3.

3.4. Geometry optimization, stability pattern

The optimizations starting from the crystallographically determined molecular structures of **1**Cl and **2** lead to global energy minima stationary points. Selected optimized bond lengths and bond angles calculated by different methods are presented in Table S1 for the sake of comparison. The normal trends observed in the crystallographic data are retained in the calculations based on various adapted methods of DFT. Calculated bond lengths and angles are in good agreement with the values obtained from the X-ray crystal structures of $\mathbf{1}^+$ and **2**. The Re–O and Re–S bond lengths are sensitive parameters employed in the methods of DFT. The calculated

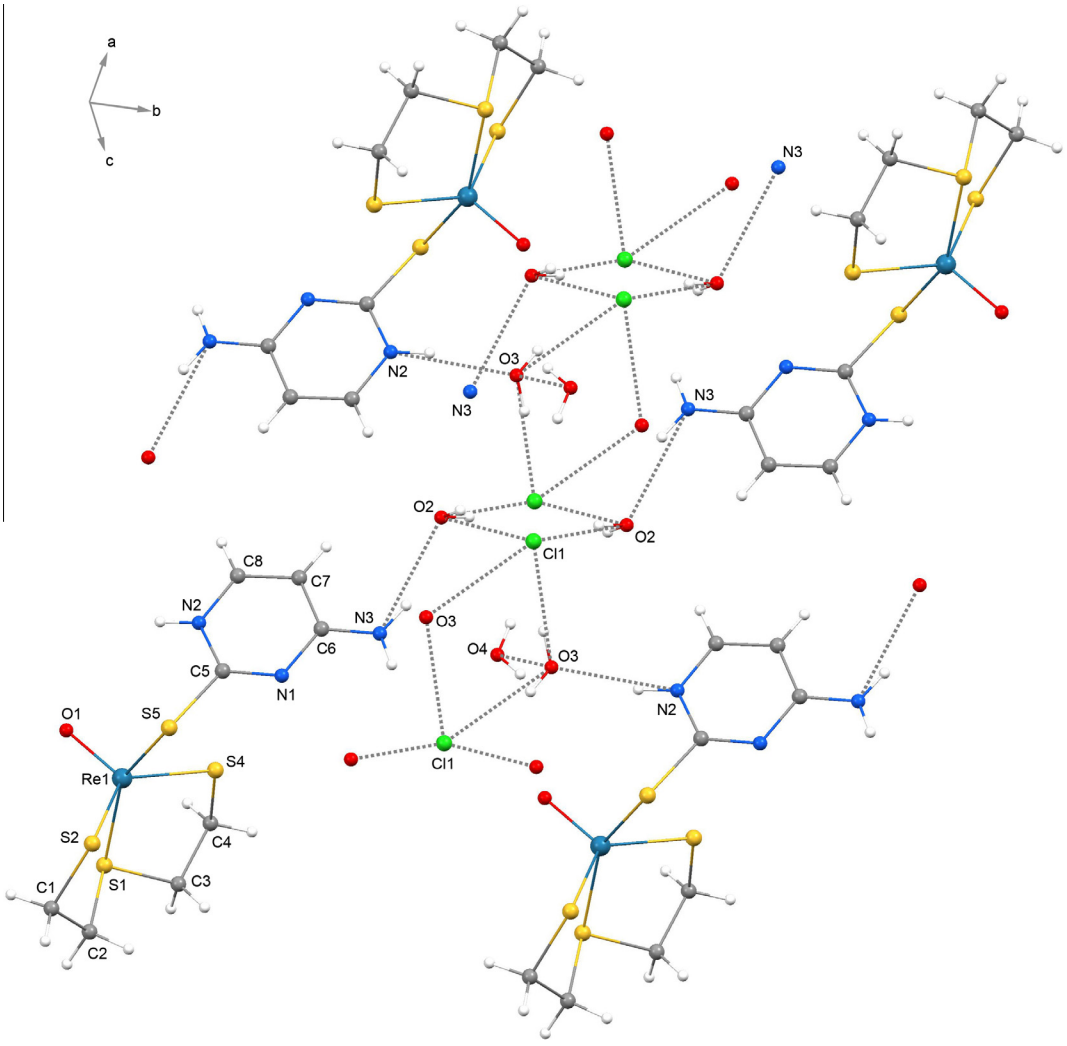

Fig. 2. A view of packing diagram of the crystal structure **1**Cl·3H_2O, C grey, N blue, O red, S yellow, Cl green and Re cyan. (For interpretation of the references to colour in this figure legend, the reader is referred to the web version of this article.)

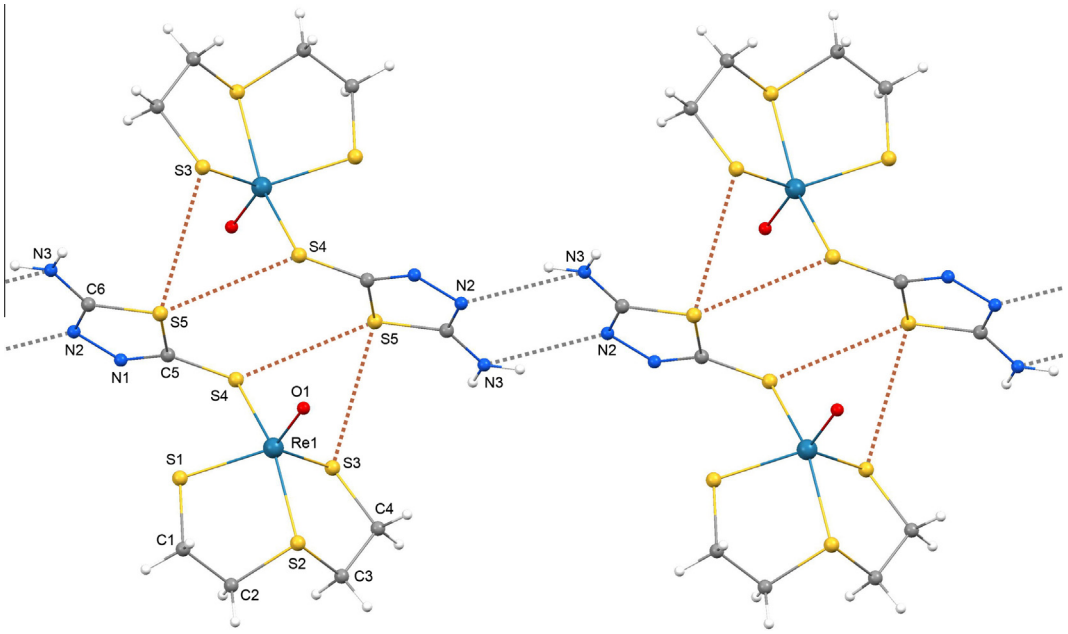

Fig. 3. Ball and stick representation of **2** displaying intermolecular NH···N hydrogen bonding (grey dotted lines) and S···S (orange dotted lines) short contract. C grey, H white, N blue, O red, S yellow, Cl green and Re cyan. (For interpretation of the references to colour in this figure legend, the reader is referred to the web version of this article.)

Re–O bond lengths are found in the range from 1.699–1.802 Å [experimental value 1.681(8) Å] for $\mathbf{1}^+$ and for **2** this range is 1.695–1.728 [experimental value 1.694(2)]. The best calculated Re–O bond lengths were obtained with the LANP1 method with a deviations of 0.018 Å for $\mathbf{1}^+$ and 0.001 for **2**. Both LANP1 and LANM reproduced exactly the same optimized data for the compound, **2**. All other methodologies are less fruitful for this bond length. Similarly, the calculated Re–S bonds are best fitted with the data generated by the STMP method. The use of the STMIDI basis sets shows an improvement of the calculated Re–S lengths compared to the LANL2DZ methods; while LANL2DZ is superior to STMIDI in case of Re–O length for both $\mathbf{1}^+$ and **2**. The STMIDI basis set in combination with PBEPBE, reproduced the experimental Re–S bond lengths most satisfactorily. However, LANP1 does not reproduce the Re–S bond lengths for both $\mathbf{1}^+$ and **2** to that optimum level. Thus we have taken recourse to the STMP method of DFT for the thermodynamic parameters for the sake of comparison of the stability and also for the assessment of electronic structures of $\mathbf{1}^+$ and **2**.

The thermodynamic parameter, reaction energy (ΔE), allows us to compare the stability sequence of a series of Re complexes both for $\mathbf{1}^+$ and **2** via the substitution reactions: $ReO(SSS)SR + L^3 \rightarrow ReOL^3SR + SSS$, with $\Delta E = [E(ReOL^3SR) + E(SSS)] - [E\{ReO(SSS)(SR)\} + E(L^3)]$ where SSS = η^3-($SCH_2CH_2SCH_2CH_2S$) and L^3 = η^3-($SCH_2CH_2OCH_2CH_2S$), η^3-($OCH_2CH_2OCH_2CH_2S$), η^3-($OCH_2CH_2SCH_2CH_2S$), η^3-($SCH_2CH_2NHCH_2CH_2S$), η^3-($OCH_2CH_2OCH_2CH_2O$), η^3-($OCH_2CH_2SCH_2CH_2O$), η^3-($OCH_2CH_2NHCH_2CH_2S$) and η^3-($OCH_2CH_2NHCH_2CH_2O$) with SR = HL^1 for $\mathbf{1}^+$ ion and SR = L^2 for **2**. The effect of substitutions on ligand frameworks were considered in the course of our calculations only in the case of tri-dentate and mono-dentate ligand-part keeping the mixed ligand (3 + 1) skeleton intact both for $\mathbf{1}^+$ and **2**. For computational simplicity, ΔE values were considered in our present studies in lieu of ΔG values. On ligand-exchange reactions of the systems, ReO(SSS)Cl and TcO(SSS)Cl; the total number of species is unaltered before and after reaction. Thus the approximation, $\Delta G \cong \Delta E$, holds good because the entropies of the reactants and products are approximately the same [24,53]. All our calculated energies for the complexes are tabulated in Table 4. Here it can be reckoned that all the ΔE values are positive, indicating

Table 4
Calculated energy of substitution (au) for the Rhenium complexes derived from $\mathbf{1}^+$ and **2** with varying tri-dentate ligand L^3 (values in au) in the gas phase.

Complexes	Energy difference (ΔE) with $\mathbf{1}^+$	Energy difference (ΔE) with **2**
ReSSS	0	0
ReSOS	0.0065127	0.0293707
ReOSS	0.0123904	0.0280668
ReSNS	0.0159088	0.0128113
ReOOS	0.0113142	0.0657512
ReOSO	0.0295655	0.0486429
ReONS	0.0324221	0.0371891
ReONO	0.0523241	0.0524850
ReOOO	0.0178638	0.0947555

that $ReO(SSS)HL^1$ and $ReO(SSS)L^2$ are the most stable congeners. Calculated energy (in au) of ligand substitution for the rhenium complexes derived from $\mathbf{1}^+$ and **2** with varying ligands in the gas phase versus the number of S atoms in tri-dentate ligands are presented in Fig. 4. The stability orders are not found to be the same for $\mathbf{1}^+$ and **2**. The determined stability order of two S donors, one S donor and zero S donor ligands runs as SOS > OSS > SNS, OOS > OSO > ONS and OOO > ONO, respectively for tri-dentate ligands in case of $\mathbf{1}^+$. For **2,** the order is just the reverse. This theoretical observation suggests that the basicity of the mono-dentate ligand, L^2 is stronger than that of HL^1. This result also predicts that complexes derived from $\mathbf{1}^+$ are thermodynamically more stable than the respective complexes derived from **2**. The only exception is noticed for the SNS ligand. In both the cases compounds derived by SSS donor ligands enjoy the maximum thermodynamic stability compared to other tri-dentate ligands.

3.5. Molecular orbital description

The partial molecular orbital energy level diagrams derived from the TD-STMP DFT calculations are shown in Figs. 5 and 6 for $\mathbf{1}^+$ and **2**. The analyses of MOs are relevant to retrospect the chemical bonding between the metal atom and the thiolato ligands and for the understanding of electronic properties. The electronic transitions and oscillator strengths for $\mathbf{1}^+$ and **2**, obtained with

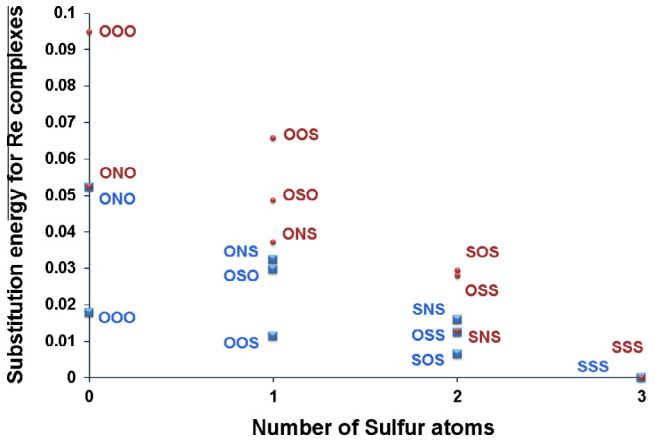

Fig. 4. Ligand substitution reaction energy (in au) versus the number of S atoms for the complexes **1**Cl (blue square) and **2** (red circle). (For interpretation of the references to colour in this figure legend, the reader is referred to the web version of this article.)

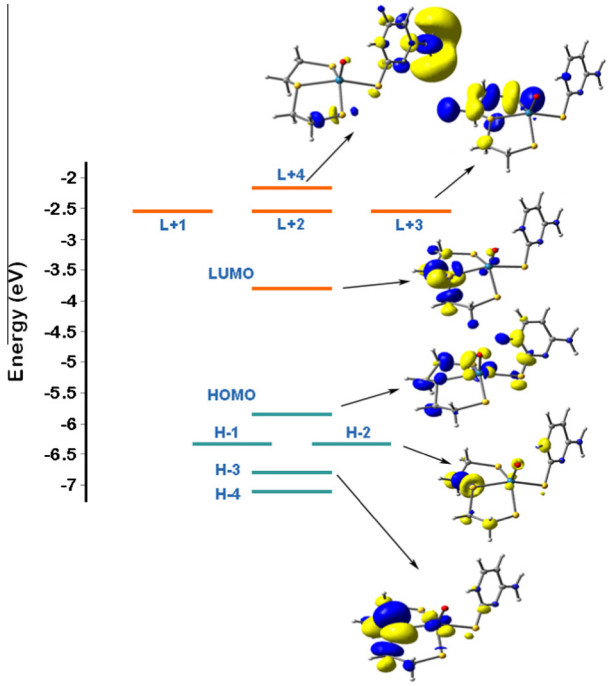

Fig. 5. The energy (eV), character and some contours of the unoccupied molecular orbitals of $\mathbf{1}^{+}$. Positive values of the orbital contour are represented in blue (0.04 au) and negative values in yellow (−0.04 au). (For interpretation of the references to colour in this figure legend, the reader is referred to the web version of this article.)

the STMP methodology, are presented in Tables 5 and 6 respectively. In both the cases strong σ- and π-donor properties of the oxido ligand destabilize the $5d_z^2$ and $5d_{xz/yz}$ orbitals within the *d* orbital manifold [28,54,55]. The electronic configuration for rhenium in $\mathbf{1}^{+}$ and **2** is formally $5d^2$. These electrons reside in a MO with a copious contribution from the $d_{x^2-y^2}$ orbital to generate a singlet ground state. The energy gaps between HOMO and LUMO are 2.048 and 2.184 eV for $\mathbf{1}^{+}$ and **2** respectively. In the cation of $\mathbf{1}^{+}$, the highest occupied molecular orbital (HOMO) has significant metallic character. It is predominantly $d_{x^2-y^2}$; while the HOMO of **2** has π-bond character resulting from mono-dentate ligand (HL^2). The highly occupied orbitals (HOMO−1, HOMO−2, HOMO−4, HOMO−5 and HOMO−7) are mostly contributed by tri-dentate ligand (SSS) orbitals and HOMO−3 is predominately contributed

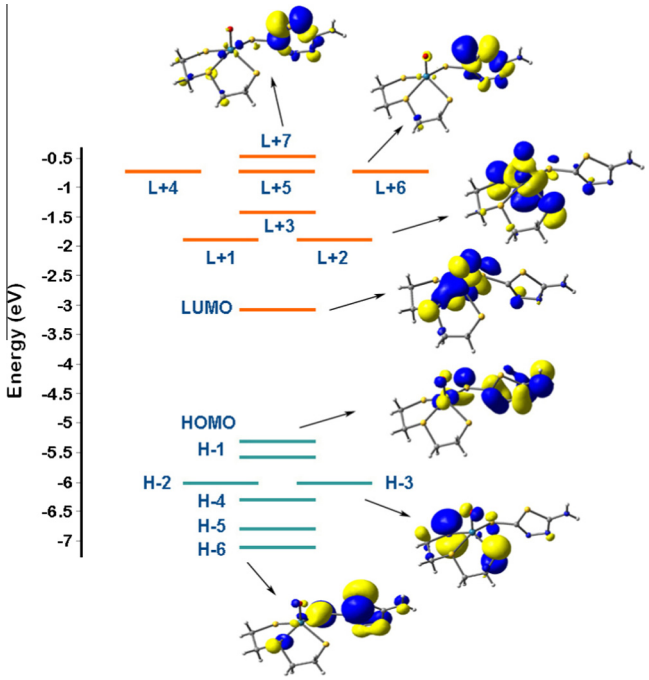

Fig. 6. The energy (eV), character and some contours of the unoccupied molecular orbitals of **2**. Positive values of the orbital contour are represented in blue (0.04 au) and negative values in yellow (−0.04 au). (For interpretation of the references to colour in this figure legend, the reader is referred to the web version of this article.)

by mono-dentate ligand (HL^1) for $\mathbf{1}^{+}$. The LUMO, LUMO+2, LUMO+3, LUMO+4 orbitals are respectively composed of d_{yz}, d_{yz}, d_{yz} and d_z^2 rhenium orbitals in anti-bonding arrangement insight into the $\mathbf{1}^{+}$. For **2,** HOMO−2 and HOMO−4 MOs are predominantly of π-bond character comprising mono-dentate ligand (HL^2). Likewise the HOMO−3 MO enjoys predominantly the π-bond character from the tri-dentate ligand (SSS) buried insight **2**. The lowest unoccupied orbitals, (LUMO+3, LUMO+4 and LUMO+5) for **2** are significantly of π-bond character arising from the mono-dentate and tri-dentate ligands. The other lowest unoccupied orbitals, (LUMO, LUMO+1 and LUMO+2) are respectively composed of d_{xz}, d_{yz} and d_z^2 orbitals of rhenium atom.

3.6. Electronic spectra

The absorption spectra for $\mathbf{1}^{+}$ and **2** are simulated in presence of the solvent employing the TD-STMP DFT methods. The findings are in good agreement with the experimental data (Figs. 7 and 8). Calculated spin-allowed singlet–singlet electronic transitions with the experimentally observed data for $\mathbf{1}^{+}$ in methanol and for **2** in DMF are summarized in Tables 5 and 6 respectively. For $\mathbf{1}^{+}$ and **2**, the high energy transitions having oscillator strengths larger than 0.0200, are incorporated. Again, the transitions only with orbital contributions larger than 10% were taken into account for both the molecules. The lowest energy absorption bands in solution were calculated at 496.43 nm for $\mathbf{1}^{+}$ and at 518.17 nm for **2**. These HOMO−1 → LUMO and HOMO → LUMO transitions are assigned as ligand-to-metal charge transfer (LMCT) transitions. The absorption bands in solution calculated at 377.82 and 415.08 nm for $\mathbf{1}^{+}$ and **2** can be described by the transitions (HOMO → LUMO+1, HOMO → LUMO+3) and (HOMO−2 → LUMO) respectively. MO analyses show that electron densities are transferred from sulfur donor atoms of ligands to the metal, which indicate that these transitions have a very strong ligand-to-metal charge transfer (LMCT) character. In the spectrum of $\mathbf{1}^{+}$, the higher energy bands

Table 5
Electronic transitions of $\mathbf{1}^{+}$ calculated in methanol using the TD-STMP DFT method.

Most important orbital excitations	λ	f	Experimental λ (ε)
H → L	548.84	0.0268	
H−1 → L	496.43	0.0034	506 (275)
H−2 → L	454.13	0.0408	
H → L+1, H → L+3	377.82	0.0100	371 (4141)
H−2 → L+3, H−2 → L+2	305.87	0.0217	
H−2 → L+4, H−4 → L+1, H−1 → L+4	277.26	0.0538	
H−9 → L	274.23	0.0416	
H−9 → L, H−3 → L+2, H−3 → L+4	273.39	0.0218	
H−3 → L+4, H−3 → L+2, H−3 → L+3	259.97	0.0305	260 (21772)
H−4 → L+2, H−4 → L+3	256.77	0.0210	
H−4 → L+3, H−4 → L+2, H−3 → L+4	256.44	0.0495	
H → L+6, H → L+7	245.70	0.0212	
H → L+7, H−7 → L+1	240.53	0.0326	
H−3 → L+5, H−4 → L+4	239.69	0.0422	242 (31967)
H−2 → L+5, H−4 → L+4, H → L+7	239.38	0.0303	
H−5 → L+4	230.85	0.0456	
H−7 → L+4, H−8 → L+3, H−9 → L+1, H−6 → L+4	221.25	0.0216	
H−9 → L+1, H−8 → L+3, H−2 → L+7	218.14	0.0638	223 (22025)
H → L+9	216.65	0.0342	

λ – wavelength (nm); ε – molar absorption coefficient ($dm^3\ mol^{-1}\ cm^{-1}$); f – oscillator strength; H – highest occupied molecular orbital; L – lowest unoccupied molecular orbital.

Table 6
Electronic transitions of **2** calculated in DMSO using the TD-STMP DFT method.

Most important orbital excitations	λ	f	Experimental λ (ε)
H → L	518.17	0.0774	501 (410)
H−2 → L	415.08	0.0264	389 (5157)
H−1 → L+3, H → L+3, H−1 → L+2	306.34	0.0275	
H−2 → L+2, H−1 → L+3, H → L+3,	296.36	0.1130	
H−3 → L+3, H−4 → L+2, H−2 → L+3	275.95	0.0287	
H−4 → L+2, H−2 → L+3, H−3 → L+2	274.28	0.0218	
H−3 → L+2, H−4 → L+2	272.11	0.0690	
H → L+5, H → L+4	266.01	0.0222	270 (14452)
H−1 → L+4	256.89	0.0220	
H−11 → L, H−1 → L+5	250.53	0.0206	

λ – wavelength (nm); ε – molar absorption coefficient ($dm^3\ mol^{-1}\ cm^{-1}$); f – oscillator strength; H – highest occupied molecular orbital; L – lowest unoccupied molecular orbital.

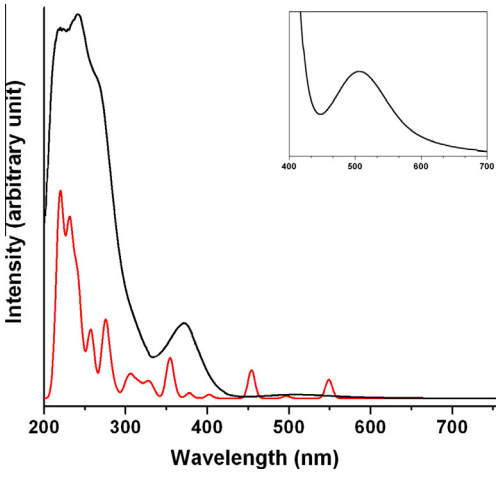

Fig. 7. The experimental (black) and calculated (red) electronic absorption spectra of **1**Cl and the magnified part is in inset. (For interpretation of the references to colour in this figure legend, the reader is referred to the web version of this article.)

at 259.97, 239.69 and 218.14 nm are assigned to the transitions: (HOMO−3 → LUMO+4, HOMO−3 → LUMO+2, HOMO−3 → LUMO+3), (HOMO−3 → LUMO+5, HOMO−4 → LUMO+4) and

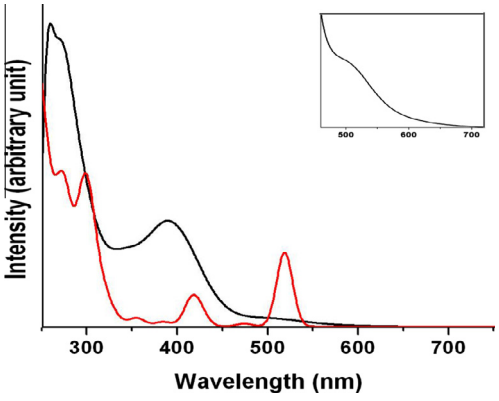

Fig. 8. The experimental (black) and calculated (red) electronic absorption spectra of **2** and the magnified part is in inset. (For interpretation of the references to colour in this figure legend, the reader is referred to the web version of this article.)

(HOMO-2 → LUMO+7, HOMO−8 → LUMO+3, HOMO−9 → LUMO+1); which can be assigned to intra-ligand or ligand to ligand transition. The calculated higher energy band at 266.01 nm for **2** can be distinguished as HOMO → LUMO+5 and HOMO → LUMO+4 ligand to ligand transition.

3.7. Electrochemistry

The electrochemical behavior of **1**Cl in acetonitrile and **2** in DMSO have been studied by cyclic voltammetry under a dry and degassed nitrogen atmosphere at a glassy carbon working electrode. The resulting cyclic voltammograms (CV) are shown in Fig. 9 and the peak potentials are tabulated in Table 7. On the positive side of the Ag/AgCl reference electrode, **1**Cl, exhibits one anodic wave (couple-I) with a peak potential of 1.654 V versus Ag/AgCl. The corresponding cathodic response is discernable in the subsequent back cycle with a peak potential value of 1.428 V versus Ag/AgCl. The ligands, HL^1 and HL^2, are electrochemically inert in the potential range of interest here. Thus this oxidation can safely be assigned as metal-centered. So, the quasi-reversible redox potential at 1.541 V versus Ag/AgCl is assigned to Re(VI)/Re(V) redox couple. This observed potential of the Re(VI)/Re(V)

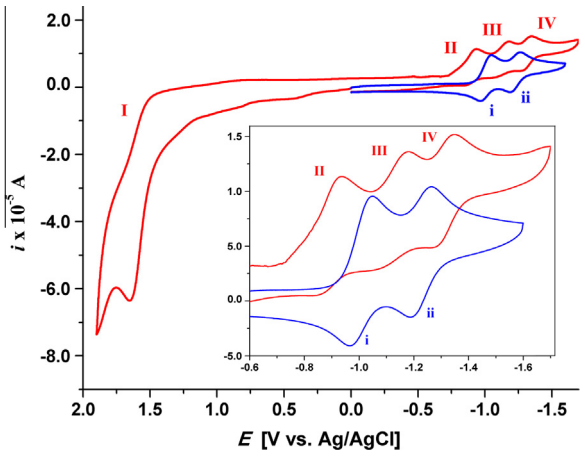

Fig. 9. Cyclic voltammogram of **1**Cl in acetonitrile (red) and **2** in DMSO (blue) at a scan rate of 100 mV s^{-1}. The concentrations of **1**Cl and **2** were 0.981 × 10^{-3} M and 1.083 × 10^{-3} M respectively. (For interpretation of the references to colour in this figure legend, the reader is referred to the web version of this article.)

Table 7
Cyclic voltammetric data for **1**Cl and **2**.

Entry	E_{pa} (V)	E_{pc} (V)	ΔE (mV)	$E^{\circ}_{1/2}$ (V)
***1**Cl*				
Couple I	1.654	1.428	226	1.541
Couple II	−0.850	−0.933	83	−0.892
Couple III	−1.066	−1.181	115	−1.124
Couple IV	−1.275	−1.345	70	−1.310
2				
Couple i	−0.968	−1.047	79	−1.008
Couple ii	−1.188	−1.264	76	−1.226

E_{pa} = anodic peak potential, E_{pc} = cathodic peak potential, $E_{1/2}$ = 0.5 (E_{pc} + E_{pa}).

redox couple is comparable to the values reported earlier [46,56,57]. To the best of our knowledge, this is the highest potential value of a Re(VI)/Re(V) couple ever reported for mixed ligand '3 + 1' systems. On the positive side of the Ag/AgCl reference electrode, **2** does not show any redox behavior. On the negative side of the reference electrode, **1**Cl displays three quasi-reversible couples (II, III and IV) at potentials −0.892, −1.124 and −1.310 V, respectively. Similarly the CV of **2** displays two quasi-reversible couples (i and ii) at potentials −1.008 and −1.226 V, respectively. The couples II, IV for **1**Cl and i, ii for **2** are reversible at low scan rates. Comparing with the literature [46], the following putative redox steps may be proposed for **1**Cl and **2**:

$$Re^{VI}O(SSS)(HL^1) + e^- \rightarrow Re^{V}O(SSS)(HL^1) \quad E_{1/2} = 1.541V$$

$$Re^{V}O(SSS)(HL^1) + e^- \rightarrow Re^{IV}O(SSS)(HL^1) \quad E_{1/2} = -0.892V$$

$$Re^{IV}O(SSS)(HL^1) + e^- \rightarrow Re^{III}O(SSS)(HL^1) \quad E_{1/2} = -1.124V$$

$$Re^{III}O(SSS)(HL^1) + e^- \rightarrow Re^{II}O(SSS)(HL^1) \quad E_{1/2} = -1.310V$$

$$Re^{V}O(SSS)(L^2) + e^- \rightarrow Re^{IV}O(SSS)(L^2) \quad E_{1/2} = -1.008V$$

$$Re^{IV}O(SSS)(L^2) + e^- \rightarrow Re^{III}O(SSS)(L^2) \quad E_{1/2} = -1.226V$$

4. Conclusions

Here we have synthesized and characterized two new '3 + 1' oxo-Re(V) complexes with 2-thiocytosine (HL^1), a sulfur heterocycle and 5-amino-1,3,4-thiadiazole-2-thiol (HL^2), an amine substituted sulfur based ligand as uni-dentate ligands. Individual reactions of chloro(3-thiapentane-1,5-dithiolato)-oxorhenium(V) [ReO(SSS)Cl] with HL^1 and HL^2 enabled us to isolate distorted square pyramidal [ReO(SSS)HL^1]Cl (**1**Cl) and [ReO(SSS)L^2] (**2**). A series of Re(V) complexes both for $\mathbf{1}^+$ and **2** involving the substitution reactions, ReO(SSS)SR + L^3 → ReOL^3SR + SSS, has been considered for thermodynamic stability calculations in gas phase. The stability-order of the tri-dentate ligands for $\mathbf{1}^+$ as determined by us is: SOS > OSS > SNS, OOS > OSO > ONS and OOO > O. For **2,** the determined order is just the reverse. The electronic structures of both $\mathbf{1}^+$ and **2** have also been calculated by C-PCM solvent model employing TD-STMP DFT and the outcome is in good harmony with the experimental findings. Furthermore, the electrochemical behaviors of **1**Cl in CH_3CN and **2** in DMSO were examined using cyclic voltammetry. Consequently, it was observed that **1**Cl exhibits rare Re(VI)/Re(V) redox couple at 1.541 V versus Ag/AgCl. Till date this is the highest potential value for a Re(VI)/Re(V) couple for mixed ligand '3 + 1' oxo-Re(V) complexes. Again, the observed potentials of 0.892, −1.124 and −1.310 V versus Ag/AgCl are assigned respectively to the Re(V)/Re(IV), Re(IV)/(III) and Re(III)/Re(II) redox couples. To the best of our knowledge, this Re(III)/Re(II) redox couple is unique and hitherto unprecedented in '3 + 1' mixed ligand oxo-rhenium(V) complexes.

Acknowledgments

Financial support (F. No. SR/FT/CS-75/2010) received from the SERB under Department of Science and Technology (DST), India, is gratefully acknowledged. J.P.N. gratefully acknowledges the University Grants Commission (UGC), New Delhi, India for financial support [F. No. 41-220/2012 (SR)].

Appendix A. Supplementary material

CCDC 953280 and 968708 contains the supplementary crystallographic data for **1**Cl·3H2O and **2**. These data can be obtained free of charge from The Cambridge Crystallographic Data Centre via www.ccdc.cam.ac.uk/data_request/cif. Supplementary data associated with this article can be found, in the online version, at http://dx.doi.org/10.1016/j.ica.2014.10.004.

References

[1] M.D. Bartholoma, A.S. Louie, J.F. Valliant, J. Zubieta, Chem. Rev. 110 (2010) 2903.
[2] J.R. Dilworth, S.J. Parrott, Chem. Soc. Rev. 27 (1998) 43.
[3] S. Liu, Chem. Soc. Rev. 33 (2004) 445.
[4] U. Abram, Rhenium, Comprehensive Coordination Chemistry II, Elsevier, 2004.
[5] W.A. Volkert, T.J. Hoffman, Chem. Rev. 99 (1999) 2269.
[6] (a) T. Fietz, H. Spies, H. Pietzsch, P. Leibnitz, Inorg. Chim. Acta 231 (1995) 233; (b) K.P. Maresca, T.M. Shoup, F.J. Femia, M.A. Burker, A. Fischman, J.W. Babich, J. Zubieta, Inorg. Chim. Acta 338 (2002) 149; (c) M.S. Papadopoulos, I.C. Pirmettis, M. Pelecanou, C.P. Raptopoulou, A. Terzis, C.I. Stassinopoulou, E. Chiotellis, Inorg. Chem. 35 (1996) 7377.
[7] (a) B. Johannsen, H.-J. Pietzsch, Eur. J. Nucl. Med. Mol. Imaging 29 (2002) 263; (b) J. Giglio, A. Rey, H. Cerecetto, I. Pirmettis, M. Papadopoulos, E. León, A. Monge, A.L. de Ceráin, A. Azqueta, M. González, Eur. J. Med. Chem. 41 (2006) 1144; (c) R. Mosi, I.R. Baird, J. Cox, V. Anastassov, B. Cameron, R.T. Skerlj, S.P. Fricker, J. Med. Chem. 49 (2006) 5262.
[8] (a) P.I.D.S. Maia, H.H. Nguyen, A. Hagenbach, S. Bergemann, R. Gust, V.M. Deflon, U. Abram, J. Chem. Soc., Dalton Trans. 42 (2013) 5111; (b) S. Chowdhury, A. Canlier, N. Koshino, Y. Ikeda, Inorg. Chim. Acta 361 (2008) 145.
[9] J. Timson, D.J. Price, J.S. Walker, Cytobios 5 (1972) 97.
[10] J.-K. Kim, Han'guk Sikp'um Yongyang Hakhoechi 10 (1997) 53.
[11] G. Lahoud, V. Timoshchuk, A. Lebedev, K. Arar, Nucleic Acids Res. 36 (2008) 6999.
[12] C. Zhao, H. Liu, Y. Zhao, Liaoning Shifan Daxue Xuebao, Ziran Kexueban 34 (2011) 482.
[13] M. Muti, A. Erdem, A.E. Karagoezler, M. Soysal, Colloids Surf., B 93 (2012) 116.

[14] M. Kavlakova, A. Bakalova, G. Momekov, D. Ivanov, Arzneimittel Forschung 62 (2012) 599.
[15] P. Kannan, S.A. John, Biosens. Bioelectron. 30 (2011) 276.
[16] W. Koch, M.C. Holthausen, A Chemist's Guide to Density Functional Theory, second ed., Wiley–VCH Verlag GmbH, 2001.
[17] J.S. Gancheff, C. Kremer, A. Kremer, O.N. Ventura, J. Mol. Struct. (Theochem.) 580 (2002) 107.
[18] J.S. Gancheff, P.A. Denis, F.E. Hahn, J. Mol. Struct. (Theochem.) 941 (2010) 1.
[19] J.S. Gancheff, A. Acosta, D. Armentano, G.D. Munno, R. Chizzone, R. Gonzalez, Inorg. Chim. Acta 387 (2012) 314.
[20] (a) B. Machura, M. Wolff, D. Tabak, Y. Ikeda, K. Hasegawa, Polyhedron 39 (2012) 76;
(b) B. Machura, I. Gryca, J.G. Małecki, F. Alonso, Y. Moglie, J. Chem. Soc., Dalton Trans. 43 (2014) 2596.
[21] B. Machura, M. Wolff, I. Gryca, Polyhedron 30 (2011) 142.
[22] J.S. Gancheff, P.A. Denis, F.E. Hahn, Spectrochim. Acta Part A: Mol. Biomol. Spectrosc. 76 (2010) 348.
[23] J.L. Smelt, C.E. Webster, E.A. Ison, Organometallics 31 (2012) 4055.
[24] B. Safi, J. Mertens, F. De Proft, R. Alberto, P. Geerlings, J. Phys. Chem. A 109 (2005) 1944.
[25] SAINT Plus, Data Reduction and Correction Program, v. 6.01, Bruker AXS. Madison, Wisconsin, USA, 1998.
[26] SADABAS v.2.01 (1998) Bruker/Siemens Area Detector Absorption Correction Program, Bruker AXS. Madison, Wisconsin, USA, 1998.
[27] G.M. Sheldrick, Acta Crysallogr., Sec. A 64 (2008) 112.
[28] J.S. Gancheff, R.Q. Albuquerque, A. Guerrero-Martínez, T. Pape, L. De Cola, F.E. Hahn, Eur. J. Inorg. Chem. 2009 (2009) 4043.
[29] J.P. Perdew, K. Burke, M. Ernzerhof, Phys. Rev. Lett. 77 (1996) 3865.
[30] C. Adamo, V. Barone, J. Chem. Phys. 110 (1999) 6158.
[31] A.D. Becke, J. Chem. Phys. 98 (1993) 1372.
[32] C. Adamo, V. Barone, J. Chem. Phys. 108 (1998) 664.
[33] J.M. Tao, J.P. Perdew, V.N. Staroverov, G.E. Scuseria, Phys. Rev. Lett. 91 (2003) 146401.
[34] P.J. Hay, W.R. Wadt, J. Chem. Phys. 82 (1985) 299.
[35] R.E. Easton, D.J. Giesen, A. Welch, C.J. Cramer, D.G. Truhlar, Theor. Chim. Acta 93 (1996) 281.
[36] (a) M. Dolg, U. Wedig, H. Stoll, H. Preuss, J. Chem. Phys. 86 (1987) 866;
(b) J.M.L. Martin, A. Sundermann, J. Chem. Phys. 114 (2001) 3408;
(c) D. Andrae, U. Häussermann, M. Dolg, H. Stoll, H. Preuss, Theor. Chim. Acta 77 (1990) 123.
[37] A. Bergner, M. Dolg, W. Kuechle, H. Stoll, M. Preuss, Mol. Phys. 80 (1993) 1431.
[38] P. Pyykkö, The Effect of Relativity in Atoms, Molecules and The Solid State, Plenum, New York, 1990.
[39] E.S. Böes, P.R. Livotto, H. Stassen, Chem. Phys. 331 (2006) 142.
[40] V. Barone, M. Cossi, J. Phys. Chem. A 102 (1998) 1995.
[41] M. Cossi, N. Rega, G. Scalmani, V. Barone, J. Comput. Chem. 24 (2003) 669.
[42] Gaussian 09, Revision C.01, M.J. Frisch, G.W. Trucks, H.B. Schlegel, G.E. Scuseria, M.A. Robb, J.R. Cheeseman, G. Scalmani, V. Barone, B. Mennucci, G.A. Petersson, H. Nakatsuji, M. Caricato, X. Li, H.P. Hratchian, A.F. Izmaylov, J. Bloino, G. Zheng, J.L. Sonnenberg, M. Hada, M. Ehara, K. Toyota, R. Fukuda, J. Hasegawa, M. Ishida, T. Nakajima, Y. Honda, O. Kitao, H. Nakai, T. Vreven, J. A. Montgomery, Jr., J.E. Peralta, F. Ogliaro, M. Bearpark, J.J. Heyd, E. Brothers, K.N. Kudin, V.N. Staroverov, R. Kobayashi, J. Normand, K. Raghavachari, A. Rendell, J.C. Burant, S.S. Iyengar, J. Tomasi, M. Cossi, N. Rega, J.M. Millam, M. Klene, J.E. Knox, J.B. Cross, V. Bakken, C. Adamo, J. Jaramillo, R. Gomperts, R.E. Stratmann, O. Yazyev, A.J. Austin, R. Cammi, C. Pomelli, J.W. Ochterski, R.L. Martin, K. Morokuma, V.G. Zakrzewski, G.A. Voth, P. Salvador, J.J. Dannenberg, S. Dapprich, A.D. Daniels, Ö. Farkas, J.B. Foresman, J.V. Ortiz, J. Cioslowski, D.J. Fox, Gaussian Inc, Wallingford CT, 2009.
[43] N.M. O'Boyle, A.L. Tenderholt, K.M. Langner, J. Comput. Chem. 29 (2008) 839.
[44] A.-R. Allouche, J. Comput. Chem. 32 (2011) 174.
[45] W.J. Geary, Coord. Chem. Rev. 7 (1971) 81.
[46] S. Chowdhury, M. Nogami, A. Canlier, Inorg. Chim. Acta 361 (2008) 1524.
[47] K.P. Maresca, F.J. Femia, G.H. Bonavia, J.W. Babich, J. Zubieta, Inorg. Chim. Acta 297 (2000) 98.
[48] E. Palma, J.D.G. Correia, A. Domingos, I. Santos, Eur. J. Inorg. Chem. (2002) 2402.
[49] K. Nakamoto, Infrared Spectra of Inorganic and Coordination Compounds, fourth ed., Wiley, New York, 1986.
[50] M.S. Papadopoulos, M. Pelecanou, I.C. Pirmettis, D.M. Spyriounis, C.P. Raptopoulou, A. Terzis, C.I. Stassinopoulou, E. Chiotellis, Inorg. Chem. 35 (1996) 4478.
[51] G.E.D. Mullen, P.J. Blower, D.J. Price, A.K. Powell, M.J. Howard, M.J. Went, Inorg. Chem. 39 (2000) 4093.
[52] S. Chowdhury, N. Koshino, A. Canlier, K. Mizuoka, Y. Ikeda, Inorg. Chim. Acta 359 (2006) 2472.
[53] W. Xiangyun, W. Yi, L. Xinqi, C. Taiwei, H. Shaowen, W. Xionghui, L. Boli, Phys. Chem. Chem. Phys. 5 (2003) 456.
[54] F.E. Inscore, R. McNaughton, B.L. Westcott, M.E. Helton, R. Jones, I.K. Dhawan, J.H. Enemark, K.L. Kirk, Inorg. Chem. 38 (1999) 1401.
[55] M.D. Carducci, C. Brown, E.I. Solomon, J.H. Enemark, J. Am. Chem. Soc. 116 (1994) 11856.
[56] S. Majumder, J.P. Naskar, S. Banerjee, A. Bhattacharya, P. Mitra, S. Chowdhury, J. Coord. Chem. 66 (2013) 1178.
[57] S. Majumder, A. Bhattacharya, J.P. Naskar, P. Mitra, S. Chowdhury, Inorg. Chim. Acta 399 (2013) 166.